

UC Davis

UC Davis Previously Published Works

Title

Microwave enhanced silica encapsulation of magnetic nanoparticles

Permalink

<https://escholarship.org/uc/item/4fz80968>

Journal

Journal of Dynamic Article LinksC< Materials Chemistry, 22(17)

Authors

Park, Jeong Chan

Gilbert, Dustin A

Liu, Kai

et al.

Publication Date

2012-03-19

Peer reviewed

Microwave enhanced silica encapsulation of magnetic nanoparticles†

Jeong Chan Park,^a Dustin A. Gilbert,^b Kai Liu^b and Angelique Y. Louie^{*a}

Received 14th December 2011, Accepted 8th March 2012

DOI: 10.1039/c2jm16595c

The surface modification of various nanoparticles with silica has been exploited to increase their utility for bioapplications. However, silica encapsulation through conventional methods requires long reaction times (hours to days). Herein, we demonstrated that uniform and spherical silica encapsulation of magnetic nanoparticles can be achieved within 10 min *via* microwave irradiation after phase transferring monodisperse magnetic nanoparticles from organic to water phase. In addition, we showed that silica shell addition through microwave synthesis is more effective than conventional heating methods, such as a hot plate. The approach that we propose may be useful in preparing multifunctional nano-probes, particularly for radiolabeling, which requires fast preparation times.

Introduction

Nanoscale materials have become an important platform in biological applications, due to their unique magnetic and/or optical properties¹ and drug loading ability.² Among nanomaterials, iron oxide based nanoparticles have been extensively studied for many applications, due to their well-established synthesis methods,^{3,4} therapeutic properties (hyperthermia)⁵ and ability to enhance magnetic resonance imaging (MRI) contrast for diagnostic applications.⁶ For biomedical application of the nanoparticles, however, they must be dispersible in aqueous media and stable in physiological environments; this is generally achieved by coating the particles with inert materials such as silica.⁷

The coating of nanomaterials with silica has the advantages of high biocompatibility, lack of toxicity, and facile surface modification. Silica encapsulation of nanomaterials can usually be attained by two approaches; a microemulsion method or a sol–gel approach. Because organic ligand-capped nanoparticles in organic solvent can be miscible with aqueous solutions to form an emulsion in the presence of surfactants, silica encapsulation through a microemulsion method, using surfactants, is useful for the coating of organic-based nanoparticles, and can produce particles which are highly monodisperse. Silica coating of superparamagnetic iron oxide (SPIO)⁸ and magnetic nanoparticles (MNs)/quantum dots (QDs),⁹ synthesized in organic phase, has been achieved through a water-in-oil microemulsion technique. However, for these particles to be used for biological applications, excess surfactant, used to make the nanoparticles

miscible, must be removed. In comparison, the sol–gel approach, based on the Stöber procedure,¹⁰ requires no surfactant and has a shorter silica encapsulation time, making it a more favorable method for biological applications. There have been several reports that describe silica based core/shell structures with silver nanowires¹¹ and water-based MNs,¹² grown by the sol–gel process. However, the sol–gel process is only applicable for water dispersible nanoparticles. Further, MNs prepared in water have poor crystallinity and polydispersity,¹³ compared to the nanoparticles generated in organic solvent.

To overcome these issues, it has been demonstrated that monodisperse MNs could be prepared in organic phase first, then transferred into water using surface modification with cetyltrimethylammonium bromide (CTAB) and subsequently encapsulated with silica through sol–gel method. This procedure often trapped multiple iron oxide cores in a single core/shell particle.¹⁴ Recently, a supercritical-fluid-assisted one pot synthesis method¹⁵ and a single-step process to coat CTAB-transferred Au nanorods and QDs with silica were also demonstrated *via* the sol–gel method.¹⁶ Tetramethylammonium hydroxide (TMAOH), another excellent phase transfer agent, has been widely used to transfer hydrophobic MNs from organic solvent to water medium.^{17,18} However, these conventional methods require rather long silica encapsulation times, ranging from hours to days.

Microwave technology has been extensively employed in organic synthesis^{19,20} and nanomaterial fabrication^{21–25} due to its many advantages, such as increased reaction rates, ability to use mild reaction conditions, and high product yield.¹⁹ In recent years, microwave approaches have been employed for silica encapsulation of bare non-magnetic nanomaterials that are water dispersible originally.^{26,27} However, it is still a challenge to achieve a uniform silica coating of monodisperse MNs with a fast encapsulation rates. To the best of our knowledge, there is no report on silica coating of organic solvent based MNs through

^aDepartment of Biomedical Engineering, University of California, Davis, California 95616, United States. E-mail: aylouie@ucdavis.edu

^bDepartment of Physics, University of California, Davis, California 95616, United States. E-mail: kailiu@ucdavis.edu

† Electronic Supplementary Information (ESI) available. See DOI: 10.1039/c2jm16595c

microwave irradiation. In this work, we report that silica encapsulation of monodisperse MN cores generated in organic phase can be achieved within minutes with the aid of microwave irradiation after TMAOH mediated phase transfer, leading to uniform and spherical core/shell architecture.

Experimental

Materials

Chemicals and reagents were purchased from Sigma-Aldrich or Fisher Scientific and used without further purification, unless otherwise noted.

Fabrication of nanoparticles

The mixture of 1 mmol of Fe(acac)₃, 5 mmol of 1,2-hexadecanediol, 3 mmol of oleic acid, 3 mmol of oleylamine and 10 mL of benzyl ether was stirred under Ar gas and heated to 200 °C for 2 h, and then 310 °C for 1 h. Cooled reaction mixture was added to 35 mL of ethanol and centrifuged at 4,400 rpm for 15 min to give black precipitates. The product was dispersed in 25 mL of hexane.

Phase transfer

~6 mg of nanoparticles in hexane solution were evaporated to remove organic solvent and 5 mL of 1 M TMAOH solution was added. The mixture was stirred for 1 h and excess TMAOH solution was discarded after collecting the magnetic nanoparticles using a permanent magnet. Ligand-exchanged nanoparticles were dispersed in 5 mL of pure water for silica coating step.

Silica encapsulation of phase transferred nanoparticles

Silica encapsulation was conducted with four different sets of samples. Each sample consisted of ligand-exchanged hydrophilic nanoparticles (~6 mg) redispersed in 5 mL of water and 10 mL of 2-propanol. These solutions were sonicated for 10 min to make them homogeneous. Different amounts (50, 150, 250 and 400 μL) of tetraethyl orthosilicate (TEOS) were added to the above solutions, respectively, then the mixtures were irradiated using a microwave (200 W, Explorer/Discover Hybrid, CEM Co.), for 10 min at 70 °C after adding 500 μL of ammonia solution (30%). For polycondensation reaction of TEOS mediated by TMAOH, hydrophilic nanoparticles were prepared with two samples, dispersed in 15 mL of water:1 M TMAOH:2-propanol at 0 : 5 : 10 and 4 : 1 : 10 ratios. After adding 400 μL (~366 mg) TEOS solution, microwave irradiation was done for 10 min at 70 °C. To compare the microwave approach with the conventional heating method, phase transferred nanoparticle solutions were prepared in water/alcohol mixture. Each of the four solutions was dispersed in 15 mL of water: 2-propanol mixture (5 : 10 ratio) containing hydrophilic iron oxide nanoparticles. The solutions were heated and stirred on a conventional bench top hot plate (Corning, Inc.) to maintain the temperature at 70 °C, and then 50, 150, 250 or 400 μL of TEOS solution was added, respectively. To these solutions 500 μL of ammonia solution (30%) was added, and then reacted for an additional 10 min at

70 °C with a hot plate. After reactions were completed the mixture was washed with ethanol (3 times) and water (2 times), respectively, by applying the centrifugation method (4,400 rpm, 15 min).

Characterization of nanoparticles

Transmission Electron Microscope (TEM) analysis was done with a CM-120 (Phillips Electronics) microscope at 80 or 120 keV. Nanoparticles were dropped on carbon coated 300 mesh copper grids (Pacific Grid Tech.) and dried at room temperature for a while for TEM analysis. Hydrodynamic diameter of hydrophobic nanoparticles was measured by a Nanotrak particle size analyzer (Microtrak, Inc.). Magnetic properties were measured using a Princeton Measurement Corp. MicroMag vibrating sample magnetometer (VSM) at room temperature.

Estimate for the number of MNs per core/shell structure

Before phase transferring and MN@SiO₂ composite MN were shown to have maximum aligned moments of 73 emu/g and 2.8 emu/g, respectively, for the ones treated with 400 μL of TEOS. Using a simple dilution model, each core/shell particle can be determined to be composed of 3.8% MN and 96.2% silica by mass. The diameter of as prepared MN was found to be 6.2 nm by X-ray diffraction, while the diameter of the composite particle was determined to be 149 nm by TEM. Using these values it is possible to estimate the number of MN cores in each MN@SiO₂ composite particle:

$$M_{MN} = \rho_{MN} V_{MN}$$

$$\text{Also, } M_{MN} = k^{MN}(\rho_{SiO_2} V_{SiO_2} + \rho_{MN} V_{MN}) = k^{MN}[\rho_{SiO_2} (V_{Total} - V_{MN}) + \rho_{MN} V_{MN}],$$

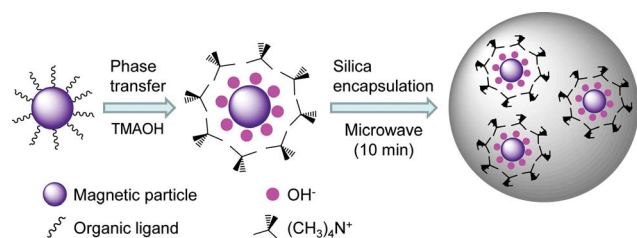
$$\text{thus } V_{MN} = (k^{MN} \rho_{SiO_2} V_{Total}) / [(1 - k^{MN}) \rho_{MN} + k^{MN} \rho_{SiO_2}],$$

$$\text{and } N_{MN} = V_{MN} / V_{Single MN}$$

where M is mass, V is volume, ρ is bulk density—5.175 g cm⁻³ for magnetite and 2.648 g cm⁻³ for silica—and *k*^{MN} is the mass percent of iron oxide—0.038 for MN. Thus each core/shell structure on average contains about 300 iron oxide nanoparticles.

Results and discussion

The overall synthetic procedure is shown in Scheme 1. First, organic ligand-capped MNs were prepared by a thermal decomposition method.³ Transmission Electron Microscope (TEM) analysis demonstrated monodisperse 5.3 ± 0.6 nm iron oxide particles, shown dispersed in organic solvent (hexane) (Fig. 1a). Dynamic light scattering (DLS) gave a particle size of 8.6 nm, reflecting the organic outer layer (Supporting



Scheme 1 Schematic illustration represents the preparation of silica encapsulated magnetic nanoparticles *via* microwave heating (10 min heating time).

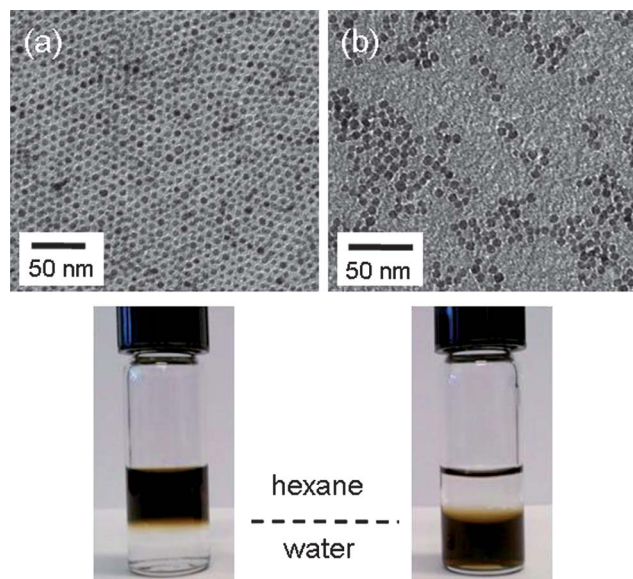


Fig. 1 TEM images (top) and photographs (bottom) of monodisperse iron oxide nanoparticles produced by thermal decomposition method. The nanoparticles were dispersed (a) in organic solution (hexane) before phase transfer and (b) in water after phase transfer using TMAOH.

Information Figure S1).²⁸ Phase transfer of hydrophobic MNs (~6 mg) into water was performed by using TMAOH in a modified literature procedure.¹⁷ As shown in Fig. 1b, the transferred nanoparticles maintained spherical morphology with aggregation (Fig. 1b, top) and dispersed well into water (bottom). After phase transfer, the size of the particles as measured by DLS increased to ~80 nm, indicating aggregation had occurred (supporting information Fig S2). It has been suggested that ligand exchange of hydrophobic MNs using TMAOH takes place through formation of an electrostatic double layer of tetramethylammonium cations and negative hydroxide ions on the surface of the nanocrystals without notable loss of crystallinity and monodispersity.^{18,29}

Silica encapsulation of phase transferred MNs was achieved in 15 mL of water/2-propanol mixture (5 : 10 ratio) through the sol-gel approach. Four different samples were prepared with different amounts (50, 150, 250 and 400 μ L) of TEOS. The samples were irradiated by microwave (10 min, 70 $^{\circ}$ C) in the presence of ammonia (30%) as a catalyst. The resulting MN/silica core/shell nanoparticles (MN@SiO₂) are shown in Fig. 2. X-ray

diffraction shows that the uncoated MNs are magnetite and/or maghemite³⁰ (Fig. 3a). Using the Scherrer equation the particle size is determined to be 6.2 nm. X-ray diffraction of MN@SiO₂ (Fig. 3b) shows a strong amorphous peak around 23 degrees, corresponding to the silica shell, and also illustrates that the encapsulated MNs remained as magnetite and/or maghemite. As the amount of TEOS is increased, the MN@SiO₂ became less aggregated and better separated, however, the thickness of the silica shell also increased, leading to larger overall size of core/shell structure. Even if multiple magnetic cores (~300 iron oxide nanoparticles per core/shell structure in some of the larger encapsulations) were encapsulated, spherical and uniform sized MN@SiO₂ were obtained through microwave synthesis with dramatically reduced time (10 min) compared to conventional approaches. The encapsulation of multiple cores in MN@SiO₂ may be the result of the high density of iron oxide nanoparticles¹² and/or increased interactions between the cores after removal of the organic capping groups from surface of MNs by TMAOH.^{14,18} MN cores were visible in low concentrations of TEOS (Fig. 2a and b), however they became blurry when the amount of TEOS was increased (Fig. 2c and d). Thus, we increased the beam energy of TEM from 80 to 120 keV in order to see the cores (Fig. 2e). Spherical SiO₂ nanoparticles without MN cores were made through microwave heating and had smaller sizes compared to MN@SiO₂ (Supporting information Fig. S3). This might be due to a larger number of nuclei formed in the absence of iron oxide. Given the avidity of TEOS for iron oxide, the iron oxide nanoparticles could act as nucleation sites for silica shell formation. In case of MN@SiO₂, various types of interconnected clusters were obtained at the lower concentrations (50, 150 and 250 μ L) of TEOS (Fig. 2a–c). In particular, the use of 50 μ L of TEOS led to chain-like core/shell structures (Fig. 2a); similar results were observed in a previous study done by a conventional heating method with a hot plate, in which polydisperse water-based ferrofluid was coated with lower amounts of TEOS.¹² Compact spherical MN@SiO₂ (149 \pm 18 nm in diameter, $n = 100$) could be obtained using 400 μ L of TEOS under our experimental conditions (Fig. 2d) and they were stable during one week in aqueous solution at room temperature (Supporting information Fig. S4). Similar observations that particle morphology grows from a fractal-like structure to compact spherical shape has been shown by a computationally simulated model³¹ and with SiO₂ particles generated by a diffusion flame reactor.³² For comparison, silica coating of organic ligand-capped MNs was performed by microwave synthesis using a microemulsion method with Triton X-100 as a surfactant. The resulting silica/MN particles showed significant aggregation, resulting in ~600 nm diameter sized clusters instead of spherical core/shell structures (data not shown).

To examine if TMAOH alone can facilitate the polycondensation reaction of TEOS to give a spherical core/shell structure in the absence of ammonia, the ligand-exchanged hydrophilic MNs were dispersed in 15 mL of water/1M TMAOH/2-propanol (0 : 5 : 10 and 4 : 1 : 10 ratio). TEOS (400 μ L) was added to the mixtures and irradiated by microwave (70 $^{\circ}$ C, 10 min) without ammonia. TEM analysis of the resulting products demonstrated that in both cases the silica layer was spread throughout the TEM grid support and around the aggregates of iron oxide nanoparticles (Supporting Information

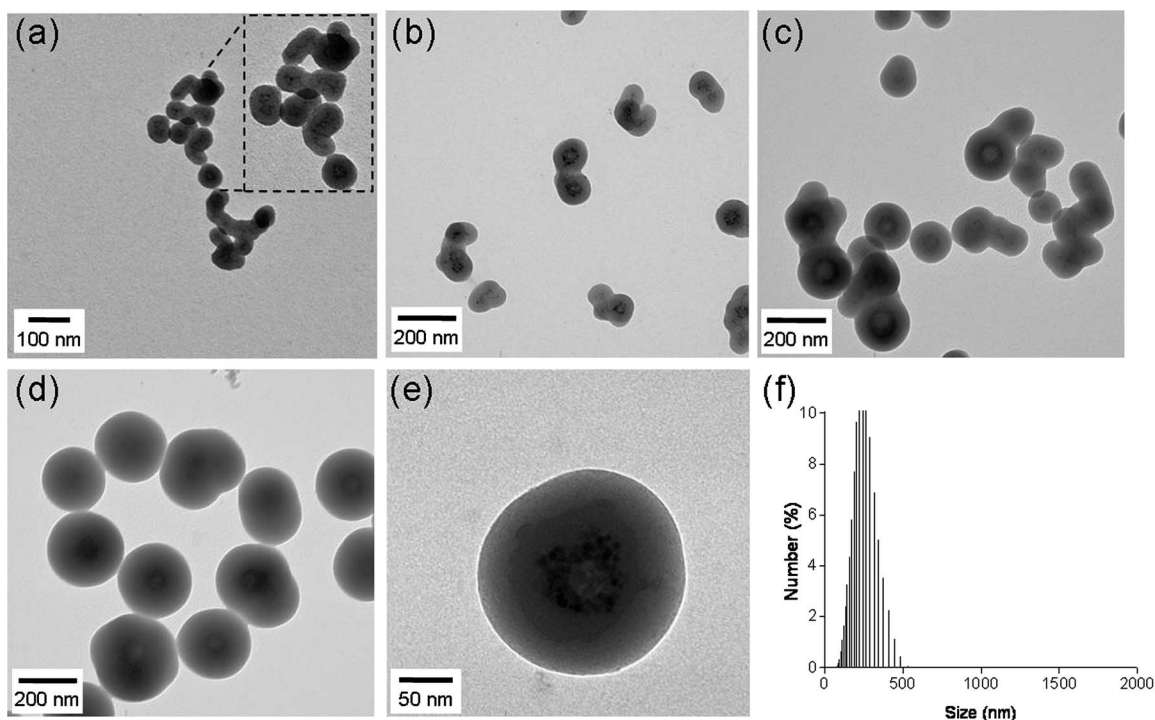


Fig. 2 TEM analysis of silica encapsulated magnetic iron oxide nanoparticles. The silica coating was generated by microwave approach (70 °C, 10 min) with increased amount [(a) 50, (b) 150, (c) 250, (d) 400 μL] of TEOS solution. Multiple magnetic cores can be observed in a and e (higher magnification at 120 keV). (f) DLS measurement of MN@SiO₂ done with 400 μL of TEOS.

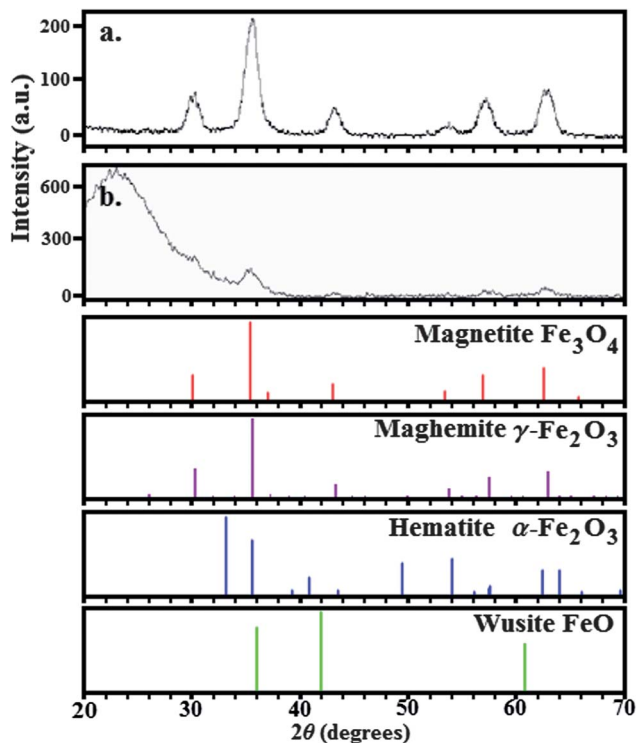


Fig. 3 X-ray diffraction patterns of (a) MN and (b) MN@SiO₂, in comparison with known iron-oxide phases.

Fig. S5). This result may have arisen from a fast and uncontrolled polycondensation reaction induced by TMAOH as a strong base.³³

To compare the microwave approach with conventional heating methods, the silica encapsulation process was carried out on a commercially available hot plate. The phase transferred MNs were dispersed in the water/2-propanol mixture and heated to 70 °C with a bench top hot plate. Four samples were prepared to which were added 50, 150, 250 or 400 μL of TEOS, and these were reacted for 10 min. As shown in Fig. 4, irregular and interconnected cluster networks were obtained for all TEOS concentrations through the conventional heating method, even at 400 μL of TEOS (Fig. 4d), compared to the uniform MN@SiO₂ that were obtained by the microwave heating approach. The beauty of the microwave approach is that silica shells could be obtained rapidly as well as more uniformly, when compared to conventional heating methods. This improvement could be the result of improved volumetric heating, accurate temperature control, selective or efficient heating of reagents having different dielectric properties, and rapid heating rate of microwave.^{19,34}

Field dependent magnetization of the microwave-generated MN@SiO₂ (400 μL TEOS) at room temperature exhibited superparamagnetic characteristics (Fig. 5a), which is critical for biomedical applications.³⁵ Maximum aligned magnetization of MN@SiO₂ at 20 kOe (~3 emu/g) is an order of magnitude less than that of phase transferred MN (22 emu/g) or the as prepared MN (73 emu/g) (Supporting Information Fig. S6), due to the silica and TMAOH addition that lowers the magnetic material content per nanoparticle. MN@SiO₂ (400 μL TEOS) demonstrate magnetic response (Fig. 5b) to external fields, which implies usefulness for various bioapplications including magnetically assisted cell separation,³⁶ drug delivery³⁷ and removal of micro-organisms.³⁸ The size of our products is

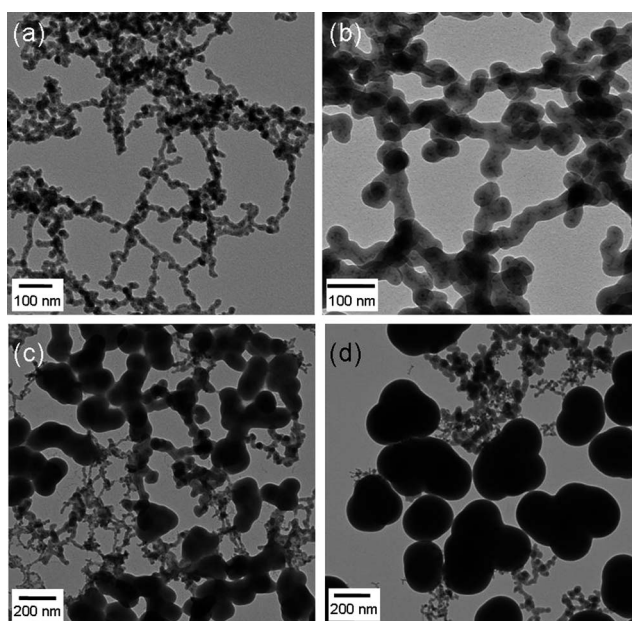


Fig. 4 TEM analysis of silica encapsulated magnetic iron oxide nanoparticles. The silica coating was generated using conventional heating methods (70 °C, 10 min, heated by hot plate) using increasing amounts ((a) 50, (b) 150, (c) 250 to (d) 400 μ L) of TEOS solution.

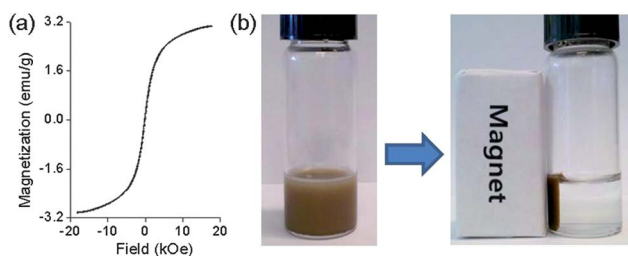


Fig. 5 (a) Magnetization curve (at room temperature) and (b) picture showing the response of silica encapsulated magnetic iron oxide nanoparticles (400 μ L TEOS) produced by microwave approach toward external permanent magnet.

comparable to commercially available magnetic nanoparticles with silica surface, such as SiMAG (0.5 μ m to 1 μ m size, Chemicell), BcMagTM (1 μ m size, Bioclone) and MagPrep[®] (0.1 μ m size, Merck), having \sim 26,³⁹ 40⁴⁰ and 88 emu/g composite,⁴¹ respectively, which are used for magnetic bioseparation.

Conclusions

We have demonstrated that uniform silica encapsulation of iron oxide nanoparticles originating from organic medium could be achieved after phase transfer using TMAOH. The resulting core/shell particles were highly spherical and monodisperse. Silica shells were obtained rapidly by using an efficient microwave irradiation method. Furthermore, the shells formed by microwave irradiation were more monodisperse than by conventional heating. The proposed approach here might be an effective method to coat multifunctional nano-platforms with silica shells, for many applications including bioseparation probes or

radiolabeling, which require rapid synthesis methods. In particular, the silica surface of magnetic responsive nanomaterials is suitable for magnetic separation of biomolecules such as proteins⁴² and DNA,⁴³ which could be efficiently adsorbed to the silica. This method can be easily extended to other organic ligand-capped nanomaterials including larger sized magnetic cores bearing higher saturation magnetization or optical nanocrystals to produce biocompatible multifunctional hybrid probes with a short synthesis time.

Acknowledgements

This work was supported by the Department of Energy (DESC0002289) and NSF (DMR-1008791). We thank G. Adamson for TEM technical assistance.

Notes and references

- 1 A. Y. Louie, *Chem. Rev.*, 2010, **110**, 3146–3195.
- 2 R. A. Petros and J. M. DeSimone, *Nat. Rev. Drug Discovery*, 2010, **9**, 615–627.
- 3 S. H. Sun, H. Zeng, D. B. Robinson, S. Raoux, P. M. Rice, S. X. Wang and G. X. Li, *J. Am. Chem. Soc.*, 2004, **126**, 273–279.
- 4 P. Jongnam, A. Kwangjin, H. Yosun, P. Je-Geun, N. Han-Jin, K. Jae-Young, P. Jae-Hoon, H. Nong-Moon and H. Taeghwan, *Nat. Mater.*, 2004, **3**, 891–895.
- 5 J.-H. Lee, J.-t. Jang, J.-s. Choi, S. H. Moon, S.-h. Noh, J.-w. Kim, J.-G. Kim, I.-S. Kim, K. I. Park and J. Cheon, *Nature Nanotechnology*, in press.
- 6 J. H. Lee, Y. M. Huh, Y. Jun, J. Seo, J. Jang, H. T. Song, S. Kim, E. J. Cho, H. G. Yoon, J. S. Suh and J. Cheon, *Nat. Med.*, 2007, **13**, 95–99.
- 7 P. Tallury, K. Payton and S. Santra, *Nanomedicine*, 2008, **3**, 579–592.
- 8 L. Chen-Wen, H. Yann, H. Jong-Kai, Y. Ming, C. Tsai-Hua, L. Yu-Shen, W. Si-Han, H. Szu-Chun, L. Hon-Man, M. Chung-Yuan, Y. Chung-Shi, H. Dong-Ming and C. Yao-Chang, *Nano Lett.*, 2006, **7**, 6.
- 9 D. K. Yi, S. T. Selvan, S. S. Lee, G. C. Papaefthymiou, D. Kundaliya and J. Y. Ying, *J. Am. Chem. Soc.*, 2005, **127**, 4990–4991.
- 10 W. Stober, A. Fink and E. Bohn, *J. Colloid Interface Sci.*, 1968, **26**, 62.
- 11 Y. D. Yin, Y. Lu, Y. G. Sun and Y. N. Xia, *Nano Lett.*, 2002, **2**, 427–430.
- 12 Y. Lu, Y. D. Yin, B. T. Mayers and Y. N. Xia, *Nano Lett.*, 2002, **2**, 183–186.
- 13 D. L. Ma, T. Veres, L. Clim, F. Normandin, J. W. Guan, D. Kingston and B. Simard, *J. Phys. Chem. C*, 2007, **111**, 1999–2007.
- 14 J. Kim, J. E. Lee, J. Lee, J. H. Yu, B. C. Kim, K. An, Y. Hwang, C. H. Shin, J. G. Park and T. Hyeon, *J. Am. Chem. Soc.*, 2006, **128**, 688–689.
- 15 E. Taboada, R. Solanas, E. Rodriguez, R. Weissleder and A. Roig, *Adv. Funct. Mater.*, 2009, **19**, 2319–2324.
- 16 I. Gorelikov and N. Matsuura, *Nano Lett.*, 2008, **8**, 369–373.
- 17 L. E. Euliss, S. G. Grancharov, S. O'Brien, T. J. Deming, G. D. Stucky, C. B. Murray and G. A. Held, *Nano Lett.*, 2003, **3**, 1489–1493.
- 18 V. Salgueirino-Maceira, L. M. Liz-Marzan and M. Farle, *Langmuir*, 2004, **20**, 6946–6950.
- 19 C. O. Kappe, *Angew. Chem., Int. Ed.*, 2004, **43**, 6250–6284.
- 20 C. H. Oh, A. K. Gupta, D. I. Park and N. Kim, *Chem. Commun.*, 2005, 5670–5672.
- 21 L. Li, H. Qian and J. Ren, *Chem. Commun.*, 2005, 528–530.
- 22 H. Hu, H. Yang, P. Huang, D. Cui, Y. Peng, J. Zhang, F. Lu, J. Lian and D. Shi, *Chem. Commun.*, 2010, **46**, 3866–3868.
- 23 I. Bilecka, I. Djerdj and M. Niederberger, *Chem. Commun.*, 2008, 886–888.
- 24 I. Bilecka and M. Niederberger, *Electrochim. Acta*, 2010, **55**, 7717–7725.
- 25 I. Bilecka and M. Niederberger, *Nanoscale*, 2010, **2**, 1358–1374.
- 26 T. Furusawa, K. Honda, E. Ukaji, M. Sato and N. Suzuki, *Mater. Res. Bull.*, 2008, **43**, 946–957.

- 27 N. M. Bahadur, T. Furusawa, M. Sato, F. Kurayama, I. A. Siddiquey and N. Suzuki, *J. Colloid Interface Sci.*, 2011, **355**, 312–320.
- 28 J. Xie, S. Peng, N. Brower, N. Pourmand, S. X. Wang and S. H. Sun, *Pure Appl. Chem.*, 2006, **78**, 1003–1014.
- 29 P. Berger, N. B. Adelman, K. J. Beckman, D. J. Campbell, A. B. Ellis and G. C. Lisensky, *J. Chem. Educ.*, 1999, **76**, 943–948.
- 30 K. Liu, L. Zhao, P. Klavins, F. E. Osterloh and H. Hiramatsu, *J. Appl. Phys.*, 2003, **93**, 7951–7953.
- 31 M. L. Eggersdorfer, D. Kadau, H. J. Herrmann and S. E. Pratsinis, *Langmuir*, 2011, **27**, 6358–6367.
- 32 A. Camenzind, H. Schulz, A. Teleki, G. Beaucage, T. Narayanan and S. E. Pratsinis, *Eur. J. Inorg. Chem.*, 2008, 911–918.
- 33 N. Ma, A. F. Marshall, S. S. Gambhir and J. H. Rao, *Small*, 2010, **6**, 1520–1528.
- 34 J. S. Schanche, *Mol. Diversity*, 2003, **7**, 293–300.
- 35 A. K. Gupta and M. Gupta, *Biomaterials*, 2005, **26**, 3995–4021.
- 36 D. S. Wang, J. B. He, N. Rosenzweig and Z. Rosenzweig, *Nano Lett.*, 2004, **4**, 409–413.
- 37 S. J. Son, J. Reichel, B. He, M. Schuchman and S. B. Lee, *J. Am. Chem. Soc.*, 2005, **127**, 7316–7317.
- 38 Y. Deng, D. Qi, C. Deng, X. Zhang and D. Zhao, *J. Am. Chem. Soc.*, 2008, **130**, 28.
- 39 U. O. Hafeli, M. A. Lobedann, J. Steingroewer, L. R. Moore and J. Riffle, *J. Magn. Magn. Mater.*, 2005, **293**, 224–239.
- 40 A. Hrdina, E. Lai, C. S. Li, B. Sadi and G. Kramer, *J. Magn. Magn. Mater.*, 2010, **322**, 2622–2627.
- 41 M. Heyd, P. Weigold, M. Franzreb and S. Berensmeier, *Biotechnology Progress*, 2009, **25**, 1620–1629.
- 42 C. H. Yu, A. Al-Saadi, S.-J. Shih, L. Qiu, K. Y. Tam and S. C. Tsang, *J. Phys. Chem. C*, 2009, **113**, 537–543.
- 43 T. Sen, A. Sebastianelli and I. J. Bruce, *J. Am. Chem. Soc.*, 2006, **128**, 7130–7131.